Chhantyal-Pun, R., Rotavera, B., McGillen, M. R., Khan, M. A. H., Eskola, A. J., Caravan, R. L., Blacker, L., Tew, D. P., Osborn, D. L., Percival, C. J., Taatjes, C. A., Shallcross, D. E., & Orr-Ewing, A. J. (2018). Criegee Intermediate Reactions with Carboxylic Acids: A Potential Source of Secondary Organic Aerosol in the Atmosphere. *ACS Earth and Space Chemistry*, *2*(8), 833-842. https://doi.org/10.1021/acsearthspacechem.8b00069

Peer reviewed version

Link to published version (if available):
10.1021/acsearthspacechem.8b00069

Criegee Intermediate Reactions with Carboxylic Acids: A Potential Source of Secondary Organic Aerosol in the Atmosphere

Rabi Chhantyal-Pun[*,†], *Brandon Rotavera*[‡,∥], *Max R. McGillen*[†], *M. Anwar H. Khan*[†], *Arkke J. Eskola*[‡,⊥], *Rebecca L. Caravan*[‡], *Lucy Blacker*[†], *David P. Tew*[†,∭], *David L. Osborn*[‡], *Carl J. Percival*[#], *Craig A. Taatjes*[‡], *Dudley E. Shallcross*[†], *Andrew J. Orr-Ewing*[*,†]

[†]School of Chemistry, University of Bristol, Cantock's Close, Bristol, BS8 1TS, [‡]Combustion Research Facility, Mail Stop 9055, Sandia National Laboratories, Livermore, CA 94551-0969, USA, [#]Jet Propulsion Laboratory, Mail Stop 183-901, 4800 Oak Drive, Pasadena, CA 92209, USA

KEYWORDS: Criegee, Carboxylic Acids, Atmospheric Chemistry, Hydroperoxide Ester, SOA

ABSTRACT: Trace atmospheric concentrations of carboxylic acids have a potent effect upon the environment, where they modulate aqueous chemistry and perturb Earth's radiative balance. Halogenated carboxylic acids are produced by the tropospheric oxidation of halocarbons and are considered persistent pollutants because of their weak tropospheric and aqueous sinks. However, recent studies reported rapid reactions between selected carboxylic acids and Criegee intermediates, which may provide an efficient gas-phase removal process. Accordingly, absolute

rate coefficients of two Criegee intermediates, CH_2OO and $(CH_3)_2COO$, with a suite of carboxylic acids (HCOOH, CH_3COOH, $CClF_2COOH$, CF_3CF_2COOH, and pyruvic acid) were measured with a view to develop a structure-activity relationship (SAR). This SAR is based upon the dipole-capture model and predicts the reactivity of many further combinations of Criegee intermediates and carboxylic acids. Complementary synchrotron-based photoionization mass spectrometry measurements demonstrate that these reactions produce stable ester adducts, with a reaction coordinate involving transfer of the acidic hydrogen from the carboxylic acid to the terminal oxygen of the Criegee intermediate. The adduct products are predicted to have low vapour pressures, and coupling of this chemistry with a global atmospheric chemistry and transport model shows significant production of secondary organic aerosol at locations rich in biogenic alkene emissions.

1. Introduction

Carboxylic acids are emitted directly to the troposphere by vegetation and combustion engines, or produced *in situ* by a range of photochemical reactions, and steady state mixing ratios of up to a few parts per billion by volume (ppbv) have been measured at various locations.[1-4] Halogenated carboxylic acids are formed from the oxidation products of anthropogenic emissions of halocarbons, [5-7] and compounds such as trifluoroacetic acid are known to be persistent in the terrestrial environment. Wet deposition is one of the main sinks for all tropospheric carboxylic acids, and contributes to the acidity of precipitation.[1] Dicarboxylic acids have low saturation vapour pressures, and are known to constitute a significant fraction of water-soluble organic aerosols in the atmosphere.[8-9]

Terrestrial biospheric sources of carboxylic acids also contribute emissions of alkenes, and ozonolysis of these alkenes is a significant source of co-located stabilized Criegee intermediates.[10] These intermediates have biradical / zwitterionic character and undergo rapid, thermalized reactions with a variety of trace atmospheric molecules, in competition with unimolecular decomposition.[11-14] Recent laboratory studies showed that their reactions with certain carboxylic acids approach or exceed the gas-kinetic collisional limit.[15-16] Complementary global modelling studies indicated that inclusion of these reactions in chemical schemes significantly lowers the predicted lifetimes and steady state concentrations of these acids in the troposphere.[15-16]

The wide range of biogenic and anthropogenic carboxylic acids emitted to the troposphere, and the variety of Criegee intermediates produced by ozonolysis of alkenes (including isoprene and terpenes), mean there are many possible combinations of reactions of atmospheric Criegee intermediates and carboxylic acids. This complexity necessitates development of structure-activity relationships (SARs) to account fully for the suite of reaction rates in atmospheric chemistry models. Here, we present a systematic study of the thermal reactions of Criegee intermediates with carboxylic acids, in which the structures of both reactants are modified by chemical substitutions to vary their reaction rates, from which we develop a useful SAR. Products of these reactions are characterized for the first time using direct measurements, and their physical properties are investigated. The results are implemented in a global atmospheric chemistry and transport model to estimate the impact of this Criegee intermediate chemistry on global secondary organic aerosol (SOA) formation.

2. Methods

2.1 Kinetic Measurements. Rates of reaction of formaldehyde oxide (CH_2OO) and acetone oxide ($(CH_3)_2COO$) Criegee intermediates with HCOOH, CH_3COOH, $CClF_2COOH$, CF_3CF_2COOH and pyruvic acid were measured in either a variable-temperature or a room-temperature flow reactor using a laser flash photolysis method described previously.[16-17] In brief, CH_2I_2 or $(CH_3)_2CI_2$ precursors were photolyzed at a laser wavelength of 355 nm in the presence of O_2 to produce the Criegee intermediates.[18-19] Details of the experimental conditions are provided in the Supporting Information. The time-dependence of Criegee intermediate absorption signal was monitored using cavity ring-down spectroscopy (CRDS), also at a wavelength of 355 nm. The carboxylic acid co-reactants were present in excess over the Criegee intermediate, such that all the measurements were conducted under pseudo-first-order conditions.

2.2. Product Measurements. The products of CH_2OO reactions with CF_3COOH, $CHCl_2COOH$, $CClF_2COOH$ and CF_3CF_2COOH were characterized using a multiplexed photoionization mass spectrometry (MPIMS) apparatus, which has been described elsewhere.[18, 20] The CH_2OO was produced using the same procedure described for kinetic measurements. The reactants and products were ionized using wavelength-selected vacuum UV photons from the Chemical Dynamics Beamline (9.0.2) of the Advanced Light Source at Lawrence Berkeley National Laboratory.

2.3. Computational Calculations. Dipole moment values were calculated at the B3LYP/AVTZ level of theory using the Gaussian 09 program.[21] Dipole moment values were also calculated with explicitly correlated coupled cluster singles, doubles and perturbative triples methods, CCSD(T)(F12*)/AVDZ//B3LYP/AVTZ, implemented in the Molpro program,[22-23] and the results are close to the B3LYP/AVTZ values calculated for the Criegee intermediates and carboxylic acids studied in this work (see Table S1 in Supporting Information). Ionization energy values were

calculated for isomers of different mass fragments observed experimentally in the reactions of CH_2OO with CF_3COOH, $CHCl_2COOH$, $CClF_2COOH$ and CF_3CF_2COOH. The composite quantum chemistry CBS-QB3 and G4 methods provided in the Gaussian 09 program were used for these calculations.[21] Intrinsic Reaction Coordinate calculations were performed for the fragmentation of $CF_3C(O)OCH_2OOH^+$ to CH_2OOH^+, CO_2 and CF_3 products. Details of various calculated structures and their conformations are provided in the Supporting Information. Vibrational frequency calculations for all the structures verified their stability.

2.4. Atmospheric Chemistry and Transport Modelling. The impact of the reactions of Criegee intermediates on concentrations of various carboxylic acids in the troposphere was assessed by incorporating the SAR predictions into the STOCHEM-CRI atmospheric chemistry and transport model.[24-26] In the model, steady state concentrations of Criegee intermediates were generated from ozonolysis of alkenes (ethene, propene, (Z)-2-butene, isoprene, α-pinene, and β-pinene). The main sink reactions of Criegee intermediates are unimolecular reaction and reaction with water and water dimer and all the reactions/rate coefficients used have been reported elsewhere.[10] The modelled Criegee intermediate concentrations were found to fall central to the range quoted by Novelli et al., but were systematically higher than those of Vereecken et al.[13, 27] There could be several causes of discrepancy between these different modelling approaches. One possibility is that the unimolecular decomposition rate coefficients for the isoprene-derived Criegee intermediates are larger in the study by Vereecken and co-workers. However, where their approach can be compared with literature measurements, there is a tendency to overestimate 1,4-hydrogen shift reaction rates [see Supplementary Table 2 of Ref. 13], and this could also be the case for the isoprene-derived Criegee intermediates. Given the apparent sensitivity of global modelling simulations to these unimolecular reaction rates, further experimental work would be useful in

resolving these differences. An updated Criegee intermediate field was generated using unimolecular reaction rate coefficients of 9000 s^{-1} for both conformers of syn-MACROO and anti-MVKOO to account for their fast interconversions. The steady state concentrations of total Criegee intermediates are not affected significantly, as both Criegee intermediates react rapidly with water in the model. The emission inventory of isoprene was also updated based on the recent study by Sindelarova and co-workers.[28]

3. Results and Discussion

3.1. Kinetics of Criegee Intermediate + Carboxylic Acid Reactions. Figure 1 shows representative decays in absorption (measured as changes in the ring-down rate coefficient) by Criegee intermediates in the presence of excess carboxylic acid, and kinetic fitting to obtain a bimolecular reaction rate coefficient. The kinetic datasets were fitted with a function incorporating simultaneous first and second order decay processes and the CRDS measurement parameters:[17]

$$\Delta\kappa(t) = \frac{k_p}{\frac{k_p}{\Delta\kappa(t_0)} e^{k_p t} - k'\left(\frac{2L}{cd}\right) + k'\left(\frac{2L}{cd}\right) e^{k_p t}} \qquad \text{(E1)}$$

Here, Δκ is the difference in the ring-down rate coefficients obtained with and without photolysis laser pulses, L is the length of the ring-down cavity, d is the overlap length of the photolysis and probe laser beams, c is the speed of light, and $k' = k/\sigma_{355nm}$ is the second order decay rate coefficient for the bimolecular self-reaction of the Criegee intermediate (k), scaled by its absorption cross section (σ_{355nm}) at the probe laser wavelength. All the experiments were performed in the variable temperature flow reactor, except for CH_2OO reactions with HCOOH, CH_3COOH, $CClF_2COOH$ and CF_3CF_2COOH which were performed in the room temperature flow reactor.[16-17] The room temperature and variable temperature flow reactors had d values of 5.7 and

7.6 cm, respectively. The parameter k_p is the sum of the pseudo first order rate coefficient for reaction with the carboxylic acid and the unimolecular rate coefficient for loss of Criegee intermediates.[17, 19] The intercept values are around an order of magnitude smaller than the smallest pseudo rate values and thus do not significantly affect the bimolecular rate coefficient measurement. The value of k' was fixed to that derived from analysis of Criegee intermediate decay traces obtained in the absence of carboxylic acids, whereas k_p and $\Delta\kappa(t_0)$ values were varied in the fits.

Table 1. Comparison of the Experimental Rate Coefficient Values with the Calculated Collision and Dipole Capture Limited Values.

Reaction	Rate Coefficient (10^{-10} cm^3 s^{-1})			
	This study	Previous studies	Collision limit[(a)]	Dipole Capture limit[(a)]
CH_2OO + HCOOH	1.14±0.06	1.1±0.1[15]	1.5	7.1
CH_2OO + CH_3COOH	1.47±0.09	1.3±0.1[15]	2.0	7.3
CH_2OO+ $CClF_2COOH$	3.3±0.2		1.9	7.1
CH_2OO+CF_3CF_2COOH	4.5±0.2		2.3	7.4
CH_2OO + Pyruvic acid	0.20±0.02		2.1	8.2
$(CH_3)_2COO$ +HCOOH	3.1±0.2		1.8	7.5
$(CH_3)_2COO$ +CH_3COOH	3.1±0.2		2.3	7.6
$(CH_3)_2COO$+$CClF_2COOH$	3.9±0.2		2.1	7.1
$(CH_3)_2COO$+CF_3CF_2COOH	4.4±0.2		2.5	7.3
$(CH_3)_2COO$ + Pyruvic acid	0.9±0.1		2.4	8.4
$(CH_3)_2COO$ +CF_3COOH		6.1±0.2[16]	2.1	7.6
CH_2OO+CF_3COOH		3.4±0.3[16]	1.9	7.6
syn-CH_3CHOO+HCOOH		2.5±0.3[15]	1.6	6.7
syn-CH_3CHOO+CH_3COOH		1.7±0.5[15]	2.1	6.9
anti-CH_3CHOO+HCOOH		5.0±3.0[15]	1.9	7.5
anti-CH_3CHOO+CH_3COOH		2.5±0.6[15]	2.4	7.7

[(a)]Further details of the methods of calculation of the collision and dipole capture limited values are provided in the Supporting Information and the main text, respectively.

The k_p value depends linearly on carboxylic acid concentration, as is exemplified in the inset to Figure 1, and the gradients of the best fit lines give the bimolecular reaction rate coefficients shown in Table 1 for various reactions studied. The 2σ statistical uncertainty of each linear fit is reported

as the error of the measurement. Any systematic errors in the experiments should be lower than this reported uncertainty. The rate coefficient values for CH_2OO + HCOOH and CH_2OO + CH_3COOH reactions obtained from this work and those reported independently by Welz *et al.* [15] are in good agreement, as shown in Table 1.

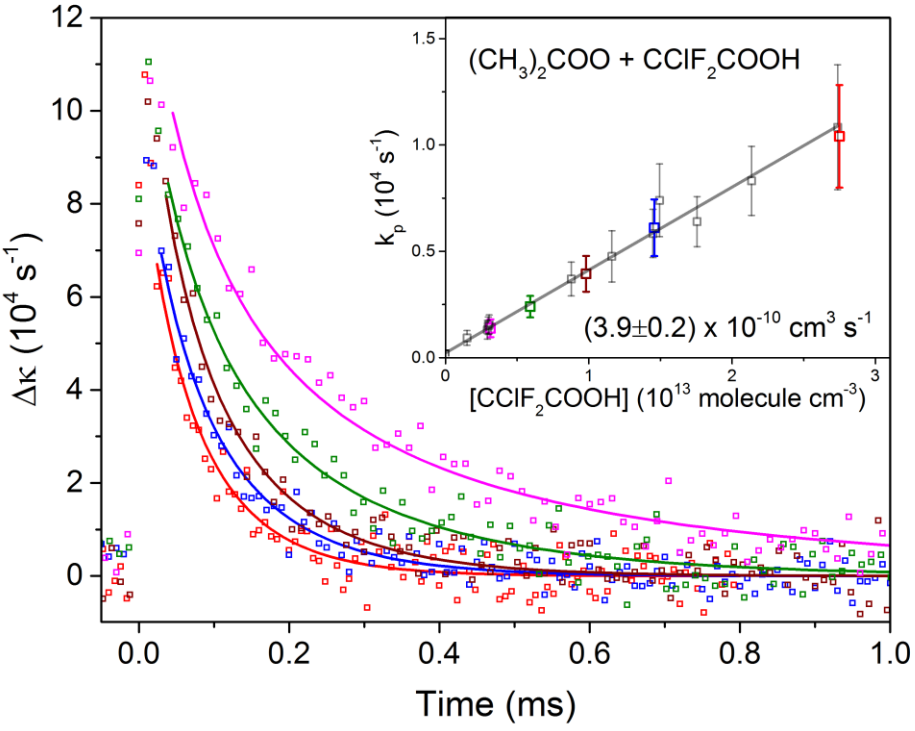

Figure 1. Representative decay traces of $(CH_3)_2COO$ absorption signal in the presence of various concentrations of $CClF_2COOH$ at 293 K and 10 Torr total pressure. The solid lines are fits obtained using equation (E1). The inset plot illustrates the pseudo first order rate coefficients obtained from these and further fits against $CClF_2COOH$ concentration. The slope of the linear fit (weighted by error bars), shown by the solid line gives a bimolecular rate coefficient value of $(3.9\pm0.2) \times 10^{-10}$ $cm^3\ s^{-1}$ for the $(CH_3)_2COO$ + $CClF_2COOH$ reaction.

The rate coefficients for most of the Criegee intermediate + carboxylic acid reactions are close to, or exceed the gas-kinetic collision limit (see Table 1), which accords with previous predictions of

a barrierless reaction involving concerted H-atom transfer and new bond formation.[16, 29-30] The Criegee intermediate + carboxylic acid reactions are instead expected to be limited by dipole-dipole attraction between the reactants, both of which have substantial dipole moments. The dipole-dipole capture limiting rate coefficient, $k_{\text{d-d}}$ in cgs units is:[31]

$$k_{d-d} = C\sqrt{\pi/\mu}\ (\mu_{D1}\mu_{D2})^{(2/3)}(k_B T)^{(-1/6)} \qquad \text{(E2)}$$

Here μ_{D1} and μ_{D2} are the dipole moments of the two reactants, μ is their reduced mass, k_B is the Boltzmann constant, T is the temperature and C is a constant which depends on the anisotropy of the capture potential. To test this proposed behaviour, dipole moment values were calculated for Criegee intermediates and various carboxylic acids at the B3LYP/AVTZ level of theory and the results are shown in Table S1 of the Supporting Information. For carboxylic acids with multiple conformers at room temperature, an effective dipole moment value was calculated by taking a weighted average based on a Boltzmann distribution at room temperature. These values were used to compute the dipole-capture limited rate coefficients reported in Table 1, where they are compared with experimental measurements.

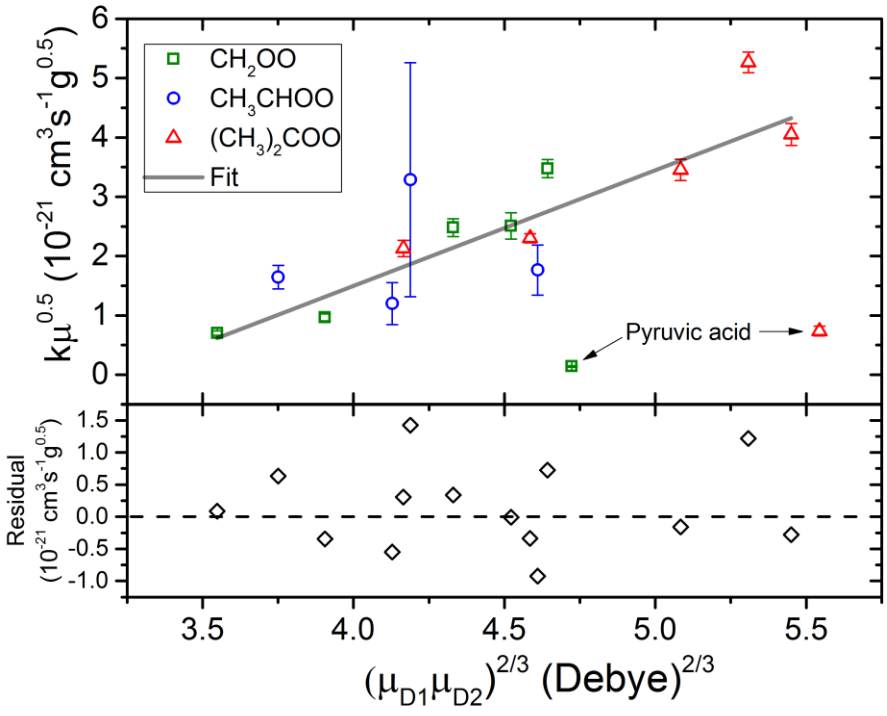

Figure 2. Structure-activity relationship based on a dipole-dipole capture model for the Criegee intermediate + carboxylic acid reaction rate coefficients. The top panel shows experimental rate coefficients for CH_2OO (green squares), CH_3CHOO (blue circles) and $(CH_3)_2COO$ (red triangles) reactions with various carboxylic acids. The solid line is a linear regression, which excludes the pyruvic acid dataset, and the best fit expression is provided in equation (E3) of the main text. CH_3CHOO and CF_3COOH rate coefficient values and uncertainties were taken from Refs 15 and 16, respectively. The bottom panel shows the residuals of the linear fit.

Figure 2 shows a plot motivated by equation (E2) and constructed from the experimental rate coefficients and computed dipole moments. A linear regression returns an adjusted R^2 value of 0.9, and provides an SAR to predict further rate coefficient values:

$$k = \mu^{-0.5}\left\{\begin{matrix}(1.9 \pm 0.2) \times 10^{-21}(\mu_{D1}\mu_{D2})^{\frac{2}{3}} \\ -(6.3 \pm 0.7) \times 10^{-21}\end{matrix}\right\} \quad \text{(E3)}$$

We note that equation (E2) predicts a zero intercept, whereas the fit in (E3) returns a negative intercept value. This discrepancy is postulated to be a consequence of the failure of the dipole capture model to account for rate coefficients in the limit of weak dipole attraction. Analysis presented in the Supporting Information suggest that the dipole-capture term becomes greater than the collision limited term for $(\mu_1\mu_2)^{2/3} > 1\ D^{4/3}$. We apply the model in the regime of $(\mu_1\mu_2)^{2/3} > 3.0\ D^{4/3}$ where the dipole capture term dominates. Furthermore, the gradient term from the fit shown in figure 2, when corrected for the chosen units, gives a C value of 6.4 which is in decent agreement with the C value of 4.08 suggested by the dipole capture model.

Although equation (E3) accounts for reactions of several carboxylic acids with Criegee intermediates, the rate coefficients for the reactions of CH_2OO and $(CH_3)_2COO$ with pyruvic acid are significantly lower than those predicted, as shown in Figure 2. These reactions are exceptional cases, in which the strong intramolecular hydrogen bonding in pyruvic acid hinders the bimolecular reaction, for which the reaction coordinate involves transfer of the hydrogen atom to the Criegee intermediate as shown in Scheme 1.

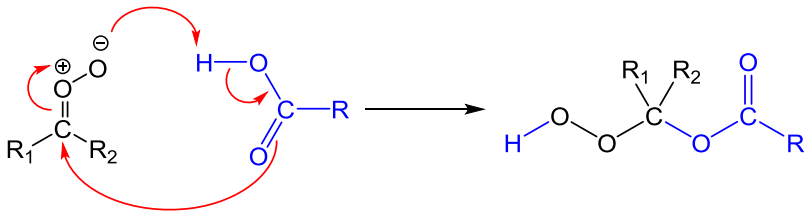

Scheme 1. Insertion reaction of a Criegee intermediate with a carboxylic acid forming a hydroperoxide ester.

With this caveat in mind, equation (E3) was used as a SAR to predict k values for reaction of Criegee intermediates, generated by ozonolysis of all the alkenes included in the STOCHEM-CRI atmospheric chemistry and transport model, with various carboxylic acids (see Tables S3 and S4 in Supporting Information) using the calculated dipole moment values. Figure 3 shows schematically the predicted reaction rate coefficients. The reduced mass, μ, value ranges from 3.82 $\times$ 10^{-23} to 1.54 $\times$ 10^{-22} g molecule^{-1} for CH_2OO + HCOOH and isopinonaldehyde oxide + pinic acid reactions, respectively. The SAR was derived using $(\mu_{D1}\mu_{D2})^{2/3}$ values in the 3.5 to 5.5 (Debye)$^{2/3}$ range, but we also apply it to values greater than 5.5 (Debye)$^{2/3}$ for e.g., pinonic and terpenylic acid reactions, for which we also expect dipole capture, and hence the SAR to operate. The $k\mu^{0.5}$ error is within $\pm 1 \times 10^{-21}$ (cm^3 s^{-1} g$^{0.5}$) as shown in Figure 2, which translates to uncertainties in k values of $\pm 1.6 \times 10^{-10}$ cm^3 s^{-1} and $\pm 0.8 \times 10^{-10}$ cm^3 s^{-1} for CH_2OO + HCOOH and isopinonaldehyde oxide + pinic acids reactions, respectively. These reactions may show some temperature dependence, but our recently reported study of the rate coefficients for reactions of CF_3COOH with CH_2OO and $(CH_3)_2COO$ suggests the variation over the range 240 – 340 K will be small (≤25%).[16]

As was noted above, the rates of reaction of pyruvic and similar acids with intramolecular hydrogen bonds cannot be reliably predicted by the SAR developed from the dipole-dipole capture model. Another class of carboxylic acids known to be important in SOA formation, and potentially prone to intramolecular H-bonding, is the dicarboxylic acids.[8] Computed optimized geometries of the most stable conformers of pyruvic and malonic acids show such intramolecular interactions (see Figure S2 in Supporting Information). In malonic acid, the labile, non-H-bonded acidic hydrogen could participate in reaction with a Criegee intermediate, whereas larger dicarboxylic acids have two labile acidic hydrogens, but lower dipole moments.[32] Thus, the reactivity of the

dicarboxylic acids is expected to be similar to regular carboxylic acids. However, dicarboxylic acids have low vapour pressures; for example, Malonic acid has a vapour pressure of 9.8×10^{-7} Torr at 298 K,[33] and the adduct products of reaction with Criegee intermediates are expected to be even less volatile, favouring condensation.

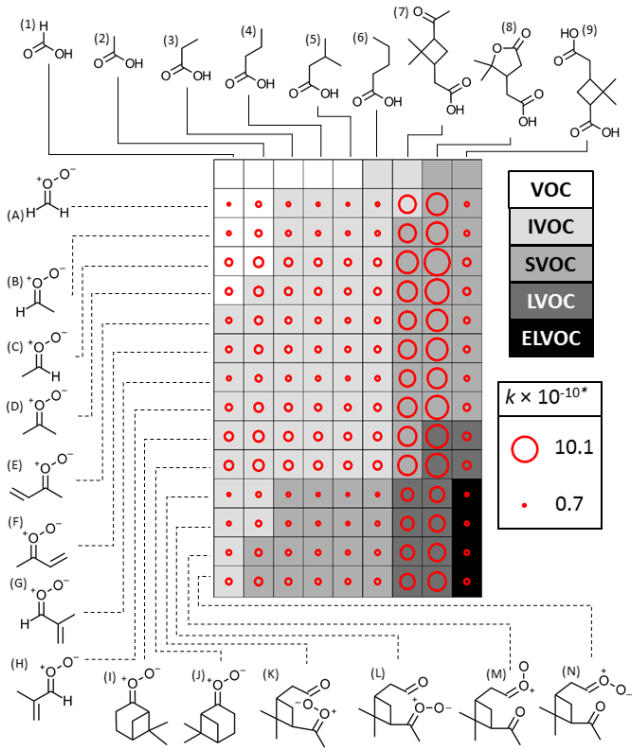

Figure 3. Predicted rate coefficients for different Criegee intermediate + carboxylic acid reactions (red circles) and volatility (grey shading) of the resultant adduct products. The diameter of each red circle indicates the magnitude of the predicted rate coefficient (*units of cm^3 s^{-1}) estimated from the structure-activity relationship. Volatilities of the products are classified according to their predicted saturation concentrations. The classification labels IVOC, SVOC, LVOC and ELVOC stand for intermediate, semi, low and extremely low volatile organic compound, respectively, and the saturation concentration ranges for these classifications are provided in Ref (34). Numerical

values of rate coefficients and saturation concentrations are provided in Tables S3 and S10 of Supporting Information.

3.2. Characterization of the Products of Criegee Intermediate + Carboxylic Acid Reactions.

Figure 4 shows photoionization energy (PIE) spectra of mass 46, 47 and 160 cations following photoionization of the CH_2OO + CF_3COOH reaction sample. The PIE spectra were obtained by integrating the cation signals over the kinetic lifetimes of the reactants and the products. Kinetic measurements were made over a sequence of photon energies to obtain a multidimensional dataset which tracks the time evolutions of the observed cations at each photon energy via time-of-flight mass spectrometry. The kinetic traces shown in the inset to Figure 4 were obtained at a fixed photoionization energy of 11.0 eV, which is above the ionization threshold of all species observed in the PIE scans. Kinetic fits were performed for the decaying and rising signals assuming single exponential behaviour. Details of the kinetic fitting procedure using an instrument response function have been described previously.[18] The best-fit rise rate constants of mass 47 and 160 cation signals were 403 ± 72 s^{-1} and 458 ± 170 s^{-1}, respectively. Similarly, the best-fit decay rate constant of mass 46 (CH_2OO) was 513 ± 23 s^{-1}, with a background wall-loss rate constant of approximately 250 s^{-1} in the absence of the carboxylic acid. The uncertainties are 2σ values of the fits. The decay and rise rate constants of mass 46, 47 and 160 cation signals are self-consistent, and mass 47 and 160 cation signals were dependent on the presence of CF_3COOH in the flow tube. Thus, mass 47 and 160 cations were assigned as the products of the CH_2OO + CF_3COOH reaction.

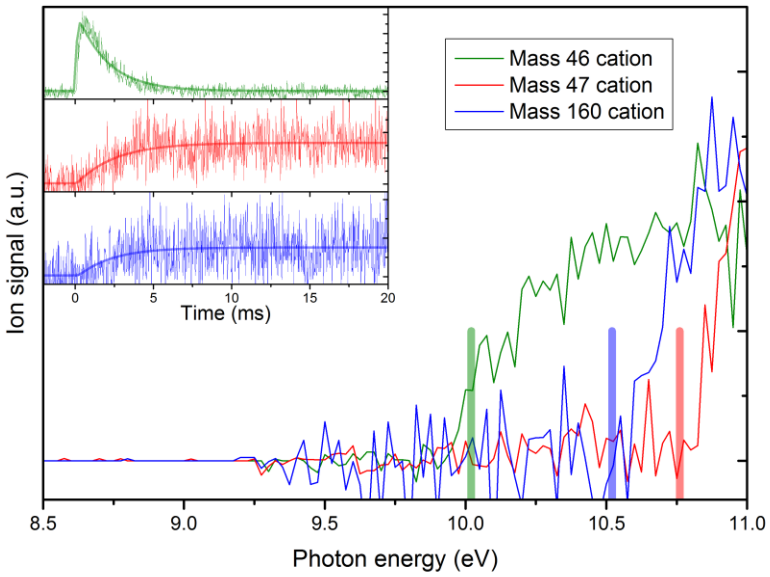

Figure 4. Product characterization from the CH_2OO + CF_3COOH reaction using multiplexed photoionization mass spectrometry. The solid lines are photoionization spectra of different mass cations observed after initiation of reaction. Kinetic measurements were made for different cations at each photon energy and integrated to obtain photoionization spectra. The vertical bars show predicted appearance energies of CH_2OO^+ (mass 46), CH_2OOH^+ (mass 47) and $CF_3COOCH_2OOH^+$ (mass 160), computed at the CBS-QB3 level of theory. The inset displays kinetic traces of the mass 46, 47 and 160 cations obtained at a photoionization energy of 11.0 eV. The smooth lines are kinetic fits to the experimental data.

Adiabatic ionization energy (AIE) values were calculated for isomers of different mass fragments observed in the CH_2OO + CF_3COOH reaction when using multiplexed photoionization mass spectrometry analysis. AIE values were also calculated for four possible mass 47 isomers, from the doublet neutral radical to either singlet or triplet cationic states (see Table S6). Only the most stable conformers were expected to be populated at room temperature for these isomers. For mass 160, only the formate isomer $CF_3C(O)OCH_2OOH$, hydroperoxymethyltrifluoroacetate (HPMTA),

was found to be stable at various levels of calculations. Multiple conformers of the formate isomer were expected to be populated at room temperature and local AIE values (ΔE_i) were calculated for excitation from the ground singlet neutral state to the ground doublet cationic state for each of these conformers. An effective AIE value, shown in Table S5, was calculated by averaging local AIE values weighted by their Boltzmann populations at 293 K. The mass 46 cation was assigned to CH_2OO based on previous studies by Welz and co-workers.[18] The mass 160 cation was assigned to HPMTA because of the close agreement of the calculated AIE with the observed appearance energy. A similar adduct, hydroperoxymethylformate (HPMF), has been observed previously from the ozonolysis of ethene to produce CH_2OO in the presence of formic acid.[35-36] Computational studies have shown that the reactions of CH_2OO with HCOOH and CF_3COOH form stable adduct products without an energy barrier.[16, 29-30]

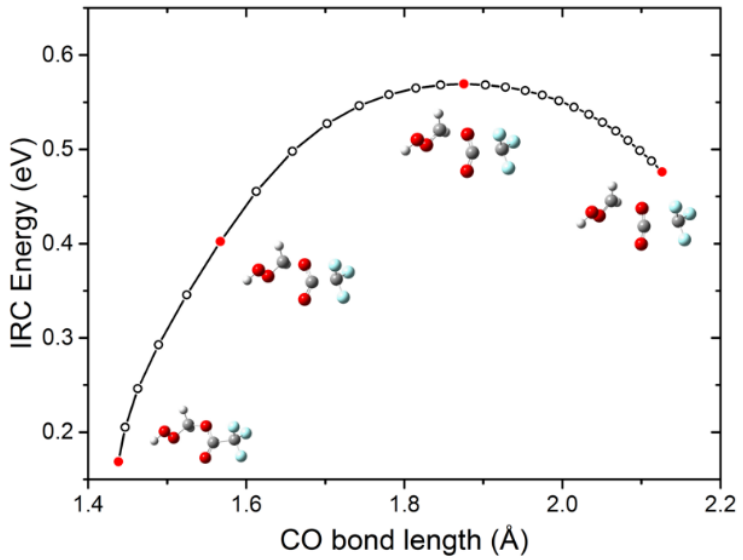

Figure 5. Intrinsic reaction coordinate for fragmentation of a $CF_3C(O)OCH_2OOH^+$ cation to CH_2OOH^+, CO_2 and CF_3 fragments, computed at the B3LYP/6-31+G(d) level of theory.

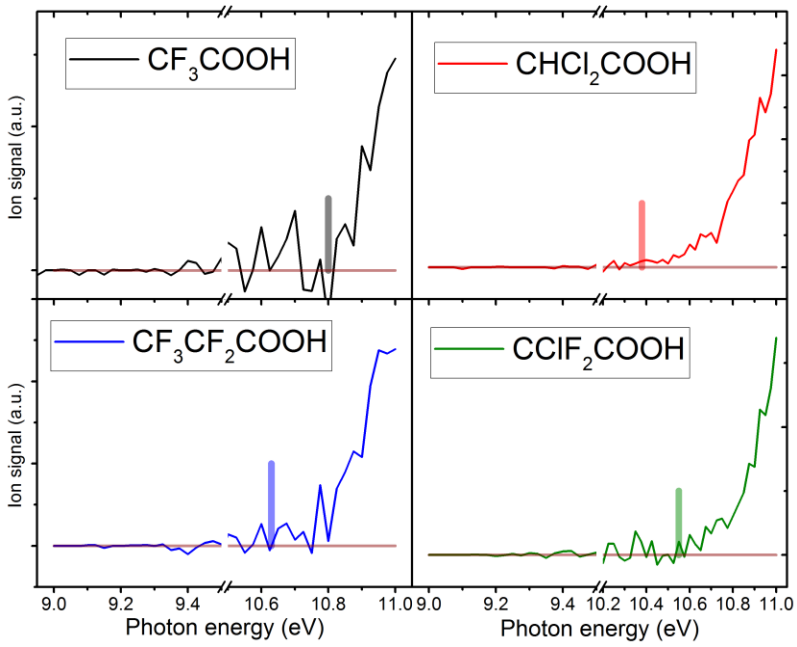

Figure 6. Photoionization energy scans of the mass 47 cation from reaction of Criegee intermediate CH_2OO with CF_3COOH, $CHCl_2COOH$, CF_3CF_2COOH and $CClF_2COOH$. The data between 9.5 and 10.5 eV are not shown in the plots to make clear the onset of the photoionization. The vertical bars show predicted thermodynamic ionization energies for formation of CH_2OOH^+ (mass 47) from the photodissociation of the adduct products.

The calculated AIE values for other possible isomers of the mass 47 cation do not match the observed appearance energy (see Table S6 in Supporting Information). Hence, thermodynamic ionization energies (TIE) were calculated for different mass 47 cations starting from HPMTA, and are listed in Table S7 in Supporting Information. These TIE values were obtained by subtracting the energy of neutral HPTMA from the energies of the possible neutral and cationic co-fragment combinations, and thus are minimum energies required for fragmentation reactions. Vibrational frequencies were verified to be positive for all the calculated geometries. TIE values were calculated for 8 possible fragmentation channels starting from HPMTA, and the TIE for the

fragmentation of $HPMTA^+$ to CH_2OOH^+, CO_2 and CF_3 products best matches the observed appearance energy. This fragmentation pathway was verified by an intrinsic reaction coordinate (IRC) calculation for the dissociation of a $CF_3COOCH_2OOH^+$ cation as shown in Figure 5. Furthermore, the sums of the AIEs and dissociation barriers are comparable to the calculated TIEs, and to the observed appearance energy values (see Table S5 in Supporting Information). Computed TIE values for analogous fragmentation pathways also compare favourably with the experimental appearance energies for CH_2OOH^+ from reactions of CH_2OO with various other halogenated acids as shown in Figure 6 and Table S8 of Supporting Information. Thus, all the reactions studied are deduced to form adduct products.

4. Atmospheric Implications

4.1. Global Carboxylic Acid Concentration. The global annual surface distribution of pinonic acid concentration was obtained using STOCHEM-CRI and is shown in Figure S4 in the Supporting Information. Pinonic acid is produced from the ozonolysis of α-pinene in the model, and partitioning onto organic aerosol to form SOA and reaction with OH radical are the two main sinks considered.[37] The rate coefficients for the production and OH loss reactions used in the model were taken from the Master Chemical Mechanism.[38] The modelled annual concentration of pinonic acid is around 1×10^8 molecule cm^{-3} (corresponding to a mixing ratio of 4 pptv) in the boreal region and parts of the USA. There are no field measurements available with which modelled pinonic acid concentrations can be compared directly. However, the study of Yatavelli et al. found that the partitioning of pinonic acid favoured the gas phase (an ~80% fraction).[39] Previously, pinonic acid was shown to comprise ~2.5% of the atmospheric organic carbon in a similar pine dominated environment.[40] Thus, the campaign average organic aerosol mass concentration of 1.96 μg m^{-3} indicates around 6×10^8 molecule cm^{-3} (24 pptv) of pinonic acid in the gas phase, which is

in reasonable agreement with modelled pinonic acid concentrations in pine-dominated areas during the summertime. Inclusion of reactions with Criegee intermediates, with rate coefficients obtained from the SAR results shown in Table S3, significantly reduces (by up to 90 percent) the modelled pinonic acid concentration, as shown in Figure 7.

The updated Criegee intermediate field and SAR predictions were also used to calculate formic acid field concentrations, with details provided in the section S7 of the Supporting Information. The model shows that the reaction with Criegee intermediates is a major sink for formic acid in the equatorial regions, in agreement with the previous study of Welz et al.[15] The percentage loss of pyruvic acid by reaction with Criegee intermediates was compared to photolytic removal (see Figure S7 of the Supporting Information), and was found to contribute up to 20 % to the overall loss. The percentage loss of trifluoroacetic acid by reaction with Criegee intermediates was also calculated, and compared to reaction with OH and deposition. The results are shown in Figure S8, and are consistent with our previous study.[16]

4.2. Global Secondary Organic Aerosol Concentration. Chamber studies have shown that ozonolysis of biogenic alkenes like isoprene and α-pinene in the presence of carboxylic acids leads to formation of adduct products in large yield.[41-42] Our observations suggest that these products could result from single step reaction of Criegee intermediates, generated during ozonolysis, with the carboxylic acids. The volatilities of the adducts were deduced from their saturation concentrations as described in detail in section S10 of the Supporting Information. The volatilities range from extremely low to intermediate, as shown in Figure 3, indicating that these adducts can readily condense to form SOA. A box model was set up to calculate SOA mass concentration resulting from the reaction of Criegee intermediates with pinonic acid. The model is summarized in Scheme 2 and couples homogeneous gas phase reactions, partitioning to an organic phase, and

deposition. The rate coefficients for Criegee intermediate reactions with pinonic acid (R1) were obtained using the SAR (Table S3 in Supporting Information) developed in this study. Rate coefficients for reaction of the adduct with OH (R2) were estimated using the EPI Suite™ software.[43] A previous study showed that reaction with OH radical is the main sink for organic hydroperoxides.[44] Reactions (R3) and (R4) describe the partitioning of gas phase adduct products into the aerosol phase, and their rate coefficients were obtained from the partitioning coefficients (Table S10 in Supporting Information) and primary organic aerosol (POA) concentrations, as described previously.[45] The partitioning coefficients were calculated using the absorptive partitioning theory of Pankow.[46] Reaction (R5) describes deposition of SOA, and a deposition lifetime of 5 days was used in the model. The concentrations of Criegee intermediates, pinonic acid, and OH were assumed to be constant in the box. To maintain constant steady state concentrations of these three species, reactions (R1) and (R2) were modified such that reactants were re-formed at the rate at which they were consumed. The steady state concentrations of various Criegee intermediates, pinonic acid, OH and POA, obtained from STOCHEM-CRI were used to calculate SOA mass concentrations at various locations, as shown in Figure 7. The concentrations for the summer and winter seasons were obtained by averaging the months of June-July-August and December-January-February, respectively. The SOA concentrations were found to reach steady state in about 20 days (Figure S11 in Supporting Information). The SOA steady state concentrations from reactions of various Criegee intermediates with pinonic acid were summed to obtain total SOA concentrations.

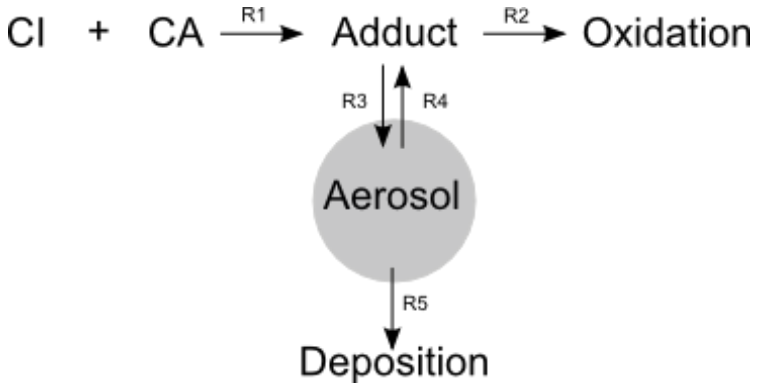

Scheme 2. Reaction of Criegee intermediates (CI) with Carboxylic Acids (CA) leading to formation of secondary organic aerosol.

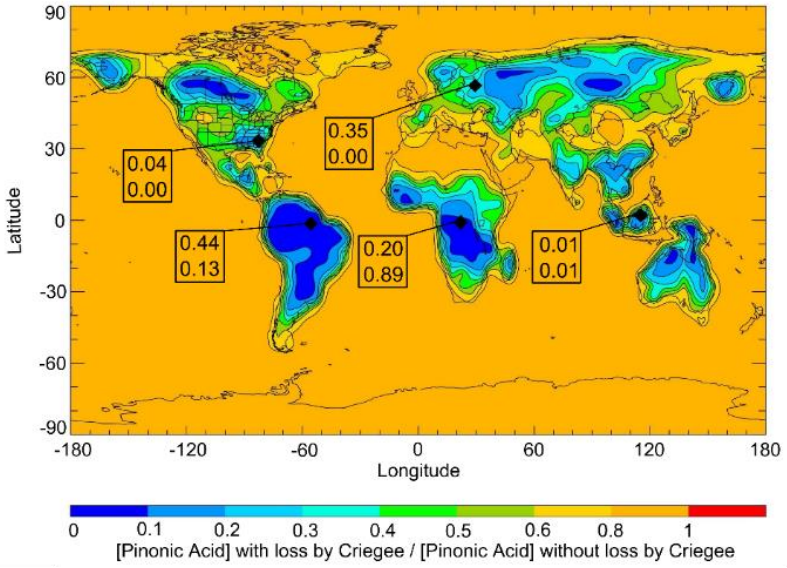

Figure 7. Modelled reduction in pinonic acid field concentration after inclusion of sink reactions with Criegee intermediates. The numbers in the black boxes give the mass concentrations (μg m^{-3}) of secondary organic aerosol (SOA) from pinonic acid + Criegee intermediate reactions in summer (June, July and August, upper) and winter (December, January and February, lower) at various locations shown by the black solid triangles. Details of the SOA calculations are provided in the text.

Figure 7 shows the predicted SOA mass concentrations from pinonic acid chemistry in the summer and winter seasons. The Congo region is predicted to have the greatest SOA mass concentrations (of up to 0.89 μg m^{-3}) from pinonic acid + Criegee intermediate chemistry, because of a combination of relatively high primary organic aerosol concentration from biomass burning and Sahara dust, high biogenic alkene emissions, and low OH concentrations. The Borneo region has a relatively low primary organic aerosol concentration, and low alkene emissions, resulting in modest overall SOA mass concentration. The boreal region exhibits large variations in SOA concentration because of strong seasonal changes in biogenic emissions. Global average organic aerosol mass concentrations of around 2.8 μg m^{-3} have been measured in various remote environments,[47] indicating that the contributions of Criegee intermediate + acid reactions may be significant in several biomes. Some products from pinonic acid have extremely low volatility (i.e., they are ELVOCs) and may therefore act as nucleating agents for atmospheric particulates, which may further increase SOA production.[48] Global models currently under-predict aerosol mass concentration, [37] and inclusion of the production of SOA from Criegee intermediate-carboxylic acid reactions should bring models into better agreement with observations.

4.3 Comparison to Other Criegee Intermediate Reactions. Reaction rates of Criegee intermediates with HNO_3 and HCl have been shown to approach or exceed the gas kinetic limit.[49-50] Both reaction types are predicted to form hydroperoxide adduct products, similar to the reactions with carboxylic acids. The hydroperoxide adducts from reaction with hydrochloric and nitric acids also have chloro and nitrate functionalities, respectively, both of which are important in atmospheric chemistry. Similar reactivity can also be expected with H_2SO_4, which has a labile hydrogen. Reactions with carboxylic acids, inorganic acids and sulphur dioxide could all be important loss processes for Criegee intermediates such as MVKOO, which can survive high

humidity and is thought to have a slow unimolecular reaction rate.[10, 13] A combined pseudo first order rate coefficient of 25 s^{-1} is estimated for loss of Criegee intermediates due to reactions with organic and inorganic acids and sulphur dioxide, assuming an overall concentration of 10 ppb and a rate coefficient of 1×10^{-10} cm^3 s^{-1}. In comparison, the predicted rate coefficients for MVKOO unimolecular reaction, and reaction with water and water dimer are 0-50, <1, and <1 s^{-1}, respectively.[10, 13]

5. Conclusions

A structure-activity relationship based on a dipole-dipole capture model accounts for the large rate coefficients for bimolecular reactions of various carboxylic acids with Criegee intermediates. However, species such as pyruvic acid, with intramolecular hydrogen bonding, react more slowly than the SAR predicts. All the reactions of carboxylic acids with Criegee intermediates, whether biogenic or anthropogenic in origin, are expected to form products with high masses and low volatilities. Complementary atmospheric chemistry and transport modelling, and SOA box modelling, using rate coefficients from the newly developed SAR, indicate that Criegee intermediate-carboxylic acid reactions may be an overlooked and potentially significant source of SOA in the atmosphere.

ASSOCIATED CONTENT

Supporting Information. Experimental conditions, dipole moment calculations (Table S1, Figures S1-S3), analysis of the onset of dipole capture behavior (Table S2), SAR predicted rate coefficients (Tables S3 and S4), AIE and TIE calculations (Tables S5-S8), modelling of pinonic acid production and loss (Figure S4), modelling of formic acid production and loss (Figures S5 and S6), modelling of pyruvic acid loss (Figure S7), modelling of trifluoroacetic acid loss (Figure

S8), predicted vapor pressures and partitioning coefficients (Tables S9 and S10) and secondary organic aerosol box modelling (Figure S9) .

Experimental data, and outputs of the quantum chemistry calculations and the SOA box model are archived in the University of Bristol's Research Data Storage Facility (DOI: 10.5523/bris.17exf0km608qe2a9uuia8e9xhz).

AUTHOR INFORMATION

Corresponding Author

*rcpchem@gmail.com

*a.orr-ewing@bristol.ac.uk

Present Addresses

‖Department of Chemistry and School of Environmental, Civil, Agricultural, and Mechanical Engineering, University of Georgia, Athens, GA 30602, USA

⊥Department of Chemistry, University of Helsinki, FI-00014, Finland

⫴Max Planck Institute for Solid State Research, Heisenbergstraβe 1, 70569 Stuttgart, Germany,

Note

The authors declare no competing financial interest.

ACKNOWLEDGMENT

This research was funded by the Natural Environment Research Council (NERC grants NE/K004905/1 and NE/P013104/1). M. R. M. is supported by Marie Sklodowska-Curie Individual

Fellowship HOMER (702794). We thank Prof G. C. Lloyd-Jones and Drs C. Nottingham and T. West (University of Edinburgh) for providing the sample of 2,2-diiodopropane. The participation of B.R., A. J. E., R. L. C., D. L. O. and C. A. T. and the development and operation of the MPIMS kinetics machine are supported by the Office of Chemical Sciences, Geosciences, and Biosciences, Office of Basic Energy Sciences, United States Department of Energy. Sandia National Laboratories is a multi-mission laboratory managed and operated by National Technology and Engineering Solutions of Sandia, LLC., a wholly owned subsidiary of Honeywell International, Inc., for the U.S. Department of Energy's National Nuclear Security Administration under contract DE-NA0003525. The Advanced Light Source is supported by the Director, Office of Science, Office of Basic Energy Sciences, of the U.S. Department of Energy under Contract No. DE-AC02-05CH11231.

REFERENCES

1. Chebbi, A.; Carlier, P., Carboxylic acids in the troposphere, occurence, sources and sinks: A review. *Atmos. Environ.* **1996,** *30*, 4233-4249.

2. Millet, D. B.; Baasandorj, M.; Farmer, D. K.; Thornton, J. A.; Baumann, K.; Brophy, P.; Chaliyakunnel, S.; Gouw, J. A. d.; Graus, M.; Hu, L.; Koss, A.; Lee, B. H.; Lopez-Hilfiker, F. D.; Neuman, J. A.; Paulot, F.; Peischl, J.; Pollack, I. B.; Ryerson, T. B.; Warneke, C.; Williams, B. J.; Xu, J., A large and ubiquitous source of atmospheric formic acid. *Atmos. Chem. Phys.* **2015,** *15*, 6283-6304.

3. Bannan, T. J.; Bacak, A.; Muller, J. B. A.; Booth, A. M.; Jones, B.; Breton, M. L.; Leather, K. E.; Ghalaieny, M.; Xiao, P.; Shallcross, D. E.; Percival, C. J., Importance of direct

anthropogenic emissions of formic acid measured by a chemical ionisation mass spectrometer (CIMS) during the Winter ClearfLo Campaign in London, January 2012. *Atmos. Environ.* **2014,** *83*, 301-310.

4. Kawamura, K.; Ng, L.-L.; Kaplan, I. R., Determination of organic acids (C1-C10) in the atmosphere, motor exhausts, and engine oils. *Environ. Sci. Technol.* **1985,** *19*, 1082-1086.

5. Bert Metz; Kuijpers, L.; Solomon, S.; Andersen, S. O.; Davidson, O.; Pons, J.; Jager, D. d.; Kestin, T.; Manning, M.; Meyer, L. *Safeguarding the Ozone Layer and the Global Climate System: Issues Related to Hydrofluorocarbons and Perfluorocarbons*; Intergovernmental Panel on Climate Change: Cambridge University Press, 2005; pp 154-155.

6. Wallington, T. J.; Andersen, M. P. S.; Nielsen, O. J., Atmospheric Chemistry of Halogenated Organic Compounds. In *Advances in Atmospheric Chemistry*, Barker, J. R.; Steiner, A. L.; Wallington, T. J., Eds. World Scientific Publishing Co. Pte. Ltd.: Singapore, 2017; Vol. 1.

7. Burkholder, J. B.; Cox, R. A.; Ravishankara, A. R., Atmospheric Degradation of Ozone Depleting Substances, Their Substitutes, and Related Species. *Chem. Rev.* **2015,** *115*, 3704-3759.

8. Bilde, M.; Barsanti, K.; Booth, M.; Cappa, C. D.; Donahue, N. M.; Emanuelsson, E. U.; McFiggans, G.; Krieger, U. K.; Marcolli, C.; Topping, D.; Ziemann, P.; Barley, M.; Clegg, S.; Dennis-Smither, B.; Hallquist, M.; Hallquist, Å. M.; Khlystov, A.; Kulmala, M.; Mogensen, D.; Percival, C. J.; Pope, F.; Reid, J. P.; Silva, M. A. V. R. d.; Rosenoern, T.; Salo, K.; Soonsin, V. P.; Yli-Juuti, T.; Prisle, N. L.; Pagels, J.; Rarey, J.; Zardini, A. A.; Riipinen, I., Saturation Vapor Pressures and Transition Enthalpies of LowVolatility Organic Molecules of Atmospheric Relevance: From Dicarboxylic Acids to Complex Mixtures. *Chem. Rev.* **2015,** *115*, 4115-4156.

9. Kawamura, K.; Bikkina, S., A review of dicarboxylic acids and related compounds in atmospheric aerosols: Molecular distributions, sources and transformation. *Atmospheric Research* **2016,** *170*, 140-160.

10. McGillen, M. R.; Curchod, B. F. E.; Chhantyal-Pun, R.; Beames, J. M.; Watson, N.; Khan, M. A. H.; McMahon, L.; Shallcross, D. E.; Orr-Ewing, A. J., Criegee intermediate-alcohol reactions, a potential source of functionalized hydroperoxides in the atmosphere. *ACS Earth Space Chem.* **2017,** *1*, 664-672.

11. Taatjes, C. A., Criegee Intermediates: What Direct Production and Detection can teach us about the reactions of carboxyl oxides. *Annu. Rev. Phys. Chem.* **2017,** *68*, 183-207.

12. Lin, J. J.-M.; Chao, W., Structure-dependent reactivity of Criegee intermediates studied with spectroscopic methods. *Chem. Soc. Rev.* **2017,** *46*, 7483-7497.

13. Vereecken, L.; Novelli, A.; Taraborrelli, D., Unimolecular decay strongly limits the atmospheric impact of Criegee intermediates. *Phys. Chem. Chem. Phys.* **2017,** *19*, 31599-31612.

14. Lester, M. I.; Klippenstein, S. J., Unimolecular Decay of Criegee Intermediates to OH Radical Products: Prompt and Thermal Decay Processes. *Acc. Chem. Res.* **2018,** *51*, 978-985.

15. Welz, O.; Eskola, A. J.; Sheps, L.; Rotavera, B.; Savee, J. D.; Scheer, A. M.; Osborn, D. L.; Lowe, D.; Booth, A. M.; Xiao, P.; Khan, M. A. H.; Percival, C. J.; Shallcross, D. E.; Taatjes, C. A., Rate Coefficients of C1 and C2 Criegee Intermediate Reactions with Formic and Acetic Acid Near the Collision Limit: Direct Kinetics Measurements and Atmospheric Implications. *Angew. Chem. Int. Ed.* **2014,** *53*, 4547-4550.

16. Chhantyal-Pun, R.; McGillen, M. R.; Beames, J. M.; Khan, M. A.; Percival, C. J.; Shallcross, D. E.; Orr-Ewing, A. J., Temperature Dependence of the Rates of Reaction of Trifluoroacetic Acid with Criegee Intermediates. *Angew. Chem. Int. Ed.* **2017,** *56*, 9044-9047.

17. Chhantyal-Pun, R.; Davey, A.; Shallcross, D. E.; Percival, C. J.; Orr-Ewing, A. J., A kinetic study of the CH_2OO Criegee intermediate self-reaction, reaction with SO_2 and unimolecular reaction using cavity ring-down spectroscopy. *Phys. Chem. Chem. Phys.* **2015,** *17*, 3617-3626.

18. Welz, O.; Savee, J. D.; Osborn, D. L.; Vasu, S. S.; Percival, C. J.; Shallcross, D. E.; Taatjes, C. A., Direct Kinetic Measurements of Criegee Intermediate (CH_2OO) Formed by Reaction of CH_2I with O_2. *Science* **2012,** *335*, 204-207.

19. Chhantyal-Pun, R.; Welz, O.; Savee, J. D.; Eskola, A. J.; Lee, E. P. F.; Blacker, L.; Hill, H. R.; Ashcroft, M.; Khan, M. A. H.; Lloyd-Jones, G. C.; Evans, L.; Rotavera, B.; Huang, H.; Osborn, D. L.; Mok, D. K. W.; Dyke, J. M.; Shallcross, D. E.; Percival, C. J.; Orr-Ewing, A. J.; Taatjes, C. A., Direct measurements of unimolecular and bimolecular reaction kinetics of the Criegee intermediate $(CH_3)_2COO$ *J. Phys. Chem. A* **2017,** *121*, 4-15.

20. Osborn, D. L.; Zou, P.; Johnsen, H.; Hayden, C. C.; Taatjes, C. A.; Knyazev, V. D.; North, S. W.; Peterka, D. S.; Ahmed, M.; Leone, S. R., The multiplexed chemical kinetic photoionization mass spectrometer: A new approach to isomer-resolved chemical kinetics. *Rev. Sci. Instrum.* **2008,** *79*, 104103.

21. Frisch, M. J.; Trucks, G. W.; Schlegel, H. B.; Scuseria, G. E.; Robb, M. A.; Cheeseman, J. R.; Scalmani, G.; Barone, V.; Mennucci, B.; Petersson, G. A.; Nakatsuji, H.; Caricato, M.; Li, X.; Hratchian, H. P.; Izmaylov, A. F.; Bloino, J.; Zheng, G.; Sonnenberg, J. L.; Hada, M.; Ehara, M.; Toyota, K.; Fukuda, R.; Hasegawa, J.; Ishida, M.; Nakajima, T.; Honda, Y.; Kitao, O.; Nakai, H.; Vreven, T.; Montgomery, J. A.; Jr., J. E. P.; Ogliaro, F.; Bearpark, M.; Heyd, J. J.; Brothers, E.; Kudin, K. N.; Staroverov, V. N.; Kobayashi, R.; Normand, J.; Raghavachari, K.; Rendell, A.; Burant, J. C.; Iyengar, S. S.; Tomasi, J.; Cossi, M.; Rega, N.; Millam, J. M.; Klene,

M.; Knox, J. E.; Cross, J. B.; Bakken, V.; Adamo, C.; Jaramillo, J.; Gomperts, R.; Stratmann, R. E.; Yazyev, O.; Austin, A. J.; Cammi, R.; Pomelli, C.; Ochterski, J. W.; Martin, R. L.; Morokuma, K.; Zakrzewski, V. G.; Voth, G. A.; Salvador, P.; Dannenberg, J. J.; Dapprich, S.; Daniels, A. D.; Farkas, Ö.; Foresman, J. B.; Ortiz, J. V.; Cioslowski, J.; Fox, D. J., *Gaussian 09, Revision D.01*. Gaussian, Inc.: Wallingford CT, 2009.

22. Werner, H.-J.; Knowles, P. J.; Knizia, G.; Manby, F. R.; Schütz, M.; Celani, P.; Györffy, W.; Kats, D.; Korona, T.; Lindh, R.; Mitrushenkov, A.; Rauhut, G.; Shamasundar, K. R.; Adler, T. B.; Amos, R. D.; Bernhardsson, A.; Berning, A.; Cooper, D. L.; Deegan, M. J. O.; Dobbyn, A. J.; Eckert, F.; Goll, E.; Hampel, C.; Hesselmann, A.; Hetzer, G.; Hrenar, T.; Jansen, G.; Köppl, C.; Liu, Y.; Lloyd, A. W.; Mata, R. A.; May, A. J.; McNicholas, S. J.; Meyer, W.; Mura, M. E.; Nicklaß, A.; O'Neill, D. P.; Palmieri, P.; Pflüger, K.; Pitzer, R.; Reiher, M.; Shiozaki, T.; Stoll, H.; Stone, A. J.; Tarroni, R.; Thorsteinsson, T.; M. Wang, *MOLPRO, version 2015.1, a package of ab initio programs.* http://www.molpro.net: 2015.

23. Hättig, C.; Tew, D. P.; Köh, A., Communications: Accurate and efficient approximations to explicitly correlated coupled-cluster singles and doubles, CCSD-F12. *J. Chem. Phys.* **2010,** *132*, 231102.

24. Utembe, S. R.; Cooke, M. C.; Archibald, A. T.; Jenkin, M. E.; Derwent, R. G.; Shallcross, D. E., Using a reduced Common Representative Intermediates (CRI v2-R5) mechanism to simulate tropospheric ozone in a 3-D Lagrangian chemistry transport model. *Atmos. Environ.* **2010,** *13*, 1609-1622.

25. Percival, C. J.; Welz, O.; Eskola, A. J.; Savee, J. D.; Osborn, D. L.; Topping, D. O.; Lowe, D.; Utembe, S. R.; Bacak, A.; McFiggans, G.; Cooke, M. C.; Xiao, P.; Archibald, A. T.; Jenkin, M. E.; Derwent, R. G.; Riipinen, I.; Mok, D. W. K.; Lee, E. P. F.; Dyke, J. M.; Taatjes,

C. A.; Shallcross, D. E., Regional and global impacts of Criegee intermediates on atmospheric sulphuric acid concentrations and first steps of aerosol formation. *Faraday Discuss.* **2013,** *165*, 45-73.

26. Khan, M. A. H.; Lyons, K.; Chhantyal-Pun, R.; McGillen, M. R.; Caravan, R. L.; Taatjes, C. A.; Orr-Ewing, A. J.; Percival, C. J.; Shallcross, D. E., Investigating the Tropospheric Chemistry of Acetic Acid Using the Global 3-D Chemistry Transport Model, STOCHEM-CRI. *J. Geophys. Res. Atmos* **2018**, DOI:10.1029/2018JD028529.

27. Novelli, A.; Hens, K.; Ernest, C. T.; Martinez, M.; Nölscher, A. C.; Sinha, V.; Paasonen, P.; Petäjä, T.; Sipilä, M.; Elste, T.; Plass-Dülmer, C.; Phillips, G. J.; Kubistin, D.; Williams, J.; Vereecken, L.; Lelieveld, J.; Harder, H., Estimating the atmospheric concentration of Criegee intermediates and their possible interference in a FAGE-LIF instrument. *Atmos. Chem. Phys.* **2017,** *17*, 7807-7826.

28. Sindelarova, K.; Granier, C.; Bouarar, I.; Guenther, A.; Tilmes, S.; Stavrakou, T.; Müller, J.-F.; Kuhn, U.; Stefani, P.; Knorr, W., Global data set of biogenic VOC emissions calculated by the MEGAN model over the last 30 years. *Atmos. Chem. Phys.* **2014,** *14*, 9317-9341.

29. Long, B.; Cheng, J.-R.; Tan, X.-f.; Zhang, W.-j., Theoretical study on the detailed reaction mechanisms of carbonyl oxide with formic acid. *J. Mol. Struct. Theochem* **2009,** *916*, 159-167.

30. Vereecken, L., The reaction of Criegee intermediates with acids and enols. *Phys. Chem. Chem. Phys.* **2017,** *19*, 28630-28640.

31. Maergoiz, A. I.; Nikitin, E. E.; Troe, J.; Ushakov, V. G., Classical trajectory and adiabatic channel study of the transition from adiabatic to sudden capture dynamics. III. Dipole–dipole capture. *J. Chem. Phys.* **1996,** *105*, 6277.

32. Nguyen, T. H.; Hibbs, D. E.; Howard, S. T., Conformations, energies, and intramolecular hydrogen bonds in dicarboxylic acids: implications for the design of synthetic dicarboxylic acid receptors. *J. Comput. Chem.* **2005,** *12*, 1233-1241.

33. Booth, A. M.; Markus, T.; McFiggans, G.; Percival, C. J.; Mcgillen, M. R.; Topping, D. O., Design and construction of a simple Knudsen Effusion Mass Spectrometer (KEMS) system for vapour pressure measurements of low volatility organics. *Atmos. Meas. Tech.* **2009,** *2*, 355-361.

34. Donahue, N. M.; Kroll, J. H.; Pandis, S. N.; Robinson, A. L., A two-dimensional volatility basis set – Part 2: Diagnostics of organic-aerosol evolution. *Atmos. Chem. Phys.* **2012,** *12*, 615-634.

35. Neeb, P.; Horie, O.; Moortgat, G. K., The Ethene-Ozone Reaction in the Gas Phase. *J. Phys. Chem. A* **1998,** *102*, 6778-6785.

36. Neeb, P.; Horie, O.; Moortgat, G. K., The nature of the transitory product in the gas-phase ozonolysis of ethene *Chem. Phys. Lett.* **1995,** *246*, 150-156.

37. Utembe, S. R.; Cooke, M. C.; Archibald, A. T.; Shallcross, D. E.; Derwent, R. G.; Jenkin, M. E., Simulating secondary organic aerosol in a 3-D Lagrangian chemistry transport model using the reduced Common Representative Intermediates mechanism (CRI v2-R5). *Atmos. Environ.* **2011,** *45*, 1604-1614.

38. The Master Chemical Mechanism. http://mcm.leeds.ac.uk/MCM.

39. Yatavelli, R. L. N.; Stark, H.; Thompson, S. L.; Kimmel, J. R.; Cubison, M. J.; Day, D. A.; Campuzano-Jost, P.; Palm, B. B.; Hodzic, A.; Thornton, J. A.; Jayne, J. T.; Worsnop, D. R.; Jimenez, J. L., Semicontinuous measurements of gas–particle partitioning of organic acids in a ponderosa pine forest using a MOVI-HRToF-CIMS. *Atmos. Chem. Phys.* **2014,** *14*, 1527-1546.

40. Maenhaut, W.; Chi, X.; Wang, W.; Cafmeyer, J.; Yasmeen, F.; Vermeylen, R.; Szmigielska, K.; Janssens, I. A.; Claeys, M., Contribution from Selected Organic Species to PM2.5 Aerosol during a Summer Field Campaign at K-Puszta, Hungary. *Atmosphere* **2017,** *8*, 221.

41. Sakamoto, Y.; Yajima, R.; Inomata, S.; Hirokawa, J., Water vapour effects on secondary organic aerosol formation in isoprene ozonolysis. *Phys. Chem. Chem. Phys.* **2017,** *19*, 3165-3175.

42. Sato, K.; Fujitani, Y.; Inomata, S.; Morino, Y.; Tanabe, K.; Ramasamy, S.; Hikida, T.; Shimono, A.; Takami, A.; Fushimi, A.; Kondo, Y.; Imamura, T.; Tanimoto, H.; Sugata, S., Lower than expected volatility of secondary organic aerosols formed during α-pinene ozonolysis. *Atmos. Chem. Phys. Discuss.* **2017**.

43. EPI Suite™ software. https://www.epa.gov/tsca-screening-tools/epi-suitetm-estimation-program-interface.

44. Khan, M. A. H.; Cooke, M. C.; Utembe, S. R.; Xiao, P.; Morris, W. C.; Derwent, R. G.; Archibald, A. T.; Jenkin, M. E.; Percival, C. J.; Shallcross, D. E., The global budgets of organic hydroperoxides for present and preindustrial scenarios. *Atmos. Environ.* **2015,** *110*, 65-74.

45. Jenkin, M. E., Modelling the formation and composition of secondary organic aerosol from - and -pinene ozonolysis using MCM v3. *Atmos. Chem. Phys.* **2004,** *4*, 1741-1757.

46. Pankow, J. F., An Absorption Model of the Gas/Aerosol Partitioning Involved in the Formation of Secondary Organic Aerosol *Atmos. Environ.* **1994,** *28*, 189-193.

47. Zhang, Q.; Jimenez, J. L.; Canagaratna, M. R.; Allan, J. D.; Coe, H.; Ulbrich, I.; Alfarra, M. R.; Takami, A.; Middlebrook, A. M.; Sun, Y. L.; Dzepina, K.; Dunlea, E.; Docherty, K.; DeCarlo, P. F.; Salcedo, D.; Onasch, T.; Jayne, J. T.; Miyoshi, T.; Shimono, A.; Hatakeyama, S.;

Takegawa, N.; Kondo, Y.; Schneider, J.; Drewnick, F.; Borrmann, S.; Weimer, S.; Demerjian, K.; Williams, P.; Bower, K.; Bahreini, R.; Cottrell, L.; Griffin, R. J.; Rautiainen, J.; Sun, J. Y.; Zhang, Y. M.; Worsnop, D. R., Ubiquity and dominance of oxygenated species in organic aerosols inanthropogenically-influenced Northern Hemisphere midlatitudes. *Geophys. Res. Lett.* **2007,** *34*, L13801.

48. Tröstl, J.; Chuang, W. K.; Gordon, H.; Heinritzi, M.; Chao Yan; Molteni, U.; Lars Ahlm; Frege, C.; Bianchi, F.; Wagner, R.; Simon, M.; Lehtipalo, K.; Williamson, C.; Craven, J. S.; Duplissy, J.; Alexey Adamov; Joao Almeida; Bernhammer, A.-K.; Breitenlechner, M.; Brilke, S.; Dias, A.; Ehrhart, S.; Flagan, R. C.; Franchin, A.; Fuchs, C.; Guida, R.; Gysel, M.; Hansel, A.; Hoyle, C. R.; Jokinen, T.; Junninen, H.; Kangasluoma, J.; Keskinen, H.; Kim, J.; Krapf, M.; Kürten, A.; Laaksonen, A.; Lawler, M.; Leiminger, M.; Mathot, S.; Möhler, O.; Nieminen, T.; Onnela, A.; Petäjä, T.; Piel, F. M.; Miettinen, P.; Rissanen, M. P.; Rondo, L.; Sarnela, N.; Schobesberger, S.; Sengupta, K.; Sipilä, M.; Smith, J. N.; Steiner, G.; Tomè, A.; Virtanen, A.; Wagner, A. C.; Weingartner, E.; Wimmer, D.; Winkler, P. M.; Penglin Ye; Carslaw, K. S.; Curtius, J.; Dommen, J.; Kirkby, J.; Kulmala, M.; Riipinen, I.; Worsnop, D. R.; Donahue, N. M.; Baltensperger, U., The role of low-volatility organic compounds in initial particle growth in the atmosphere. *Nature* **2016,** *533*, 527-531.

49. Foreman, E. S.; Kapnas, K. M.; Murray, C., Reactions between Criegee Intermediates and the Inorganic Acids HCl and HNO_3:Kinetics and Atmospheric Implications. *Angew. Chem. Int. Ed.* **2016,** *55*, 10419-10422.

50. Raghunath, P.; Lee, Y.-P.; Lin, M. C., Computational Chemical Kinetics for the Reaction of Criegee Intermediate CH_2OO with HNO_3 and Its Catalytic Conversion to OH and HCO. *J. Phys. Chem. A* **2017,** *121*, 3871-3878.

SYNOPSIS (Word Style “SN_Synopsis_TOC”). If you are submitting your paper to a journal that requires a synopsis, see the journal’s Instructions for Authors for details.